Article

Collector Efficiency in Downward-Type Internal-Recycle Solar Air Heaters with Attached Fins

Ho-Ming Yeh and Chii-Dong Ho *

Energy and Opto-Electronic Materials Research Center, Department of Chemical and Materials Engineering, Tamkang University, Tamsui, New Taipei 251, Taiwan;
E-Mail: hmyeh@mail.tku.edu.tw

* Author to whom correspondence should be addressed; E-Mail: cdho@mail.tku.edu.tw;
Tel.: +886-2-26215656, ext. 2724; Fax: +886-2-26209887.

Abstract: The internal-recycle operation effect on collector efficiency in downward-type rectangular solar air heaters with attached fins is theoretically investigated. It is found that considerable collector efficiency is obtainable if the collector has attached fins and the operation is carried out with internal recycling. The recycling operation increases the fluid velocity to decrease the heat transfer resistance, compensating for the undesirable effect of decreasing the heat transfer driving force (temperature difference) due to remixing. The attached fins provide an enlarged heat transfer area. The order of performance in a device of same size is: double pass with recycle and fins > double pass with recycle but without fins > single pass without recycle and fins.

Nomenclature:

A_c = surface area of the absorbing plate = BL (m^2)

A_f = total surface area of fins (m^2)

B = the width of absorber surface area = nw_1 (m)

C_p = specific heat of air at constant pressure (J/kg·K)

D_e = equivalent diameter of the channel (m)

E = further improvement of collector efficiency, defined by Equation (41)

F_1, F_2 = collector efficiency factors for subchannels 1 and 2, respectively

H = height of the air tunnel in the solar collector, or the distance between glass cover and absorbing plate (m)

h = convective heat-transfer coefficient for fluid flowing over the plate of duct ($W/m^2\ K$)

$h_{p\text{-}c}$ = convection coefficient between the plate and glass ($W/m^2\ K$)

$h_{p\text{-}R}$ = radiant heat-transfer coefficient between two parallel plates ($W/m^2\ K$)

$h_{r,c-a}$ = radiation coefficient from the glass to the air ($W/m^2\ K$)

$h_{r,p\text{-}c}$ = radiation coefficient from the plate to the glass ($W/m^2\ K$)

h_w = convective feat-transfer coefficient between glass cover and ambient ($W/m^2\ K$)

I = improvement of collector efficiency in the recycle device without fins, Equation (39)

I_f = improvement of collector efficiency in the recycle device with attached fins, Equation (40)

I_0 = solar radiation incident (W/m^2)

k = thermal conductivity of air ($W/m^2\ K$)

k_s = thermal conductivity of absorbing plate and fins ($W/m^2\ K$)

L = collector length (m)

$\dot{m}$ = mass-flow rate of air (kg/s)

n = fin number

Nu = Nusselt number

Q_u = useful gain of energy carried away by air per unit time (W)

R = reflux ratio

Re = Reynolds number of flow channel

T = temperature (K)

t = fin thickness

U_t = loss coefficient from the top of solar collector to the ambient($W/m^2\ K$)

$\bar{v}$ = Average air velocity in the flow channel (m/s)

V = wind velocity (m/s)

w_1 = distance between fins (m)

w_2 = height of fin (m)

z = axis along the flow direction (m)

Greek Letters

η_c = collector efficiency of a solar air collector with recycle but without fins

$\bar{\eta}_c$ = collector efficiency of a single-pass solar air collector without recycle and fins

η_{cf} = collector efficiency of a solar air collector with recycle and fins

η_f = fin efficiency

σ = the Stefan-Boltzmann constant ($W/m^2\ K^4$)

ε_g = emissivity of glass cover

ε_p = emissivity of absorbing plate

ε_R = emissivity of bottom plate

τ_g = transmittance of glass cover

α_p = absorptivity of the absorbing plate

ϕ = modified factor for attached fins, defined by Equation (4)

Subscripts

a = ambient

f = fluid

i = inlet

m = mean value

o = outlet at subchannel 1 ($z = L$)

p = absorbing plate

R = bottom plate

1,2 = subchannel 1, subchannel 2

Superscripts

0 = mixed

$'$ = Outlet at the first pass or inlet at subchannel 2 ($z = L$)

1. Introduction

Solar air heaters in which energy is transferred from a distant radiant energy source directly into air [1,2], can be employed for drying, supplying fresh air to hospitals, and paint spraying operations [3]. The flat-plate solar air heater is a simple device consisting of one or more glasses or transparent material covers situated above an absorbing plate with the air flowing either over or under the absorbing plates [4–6].
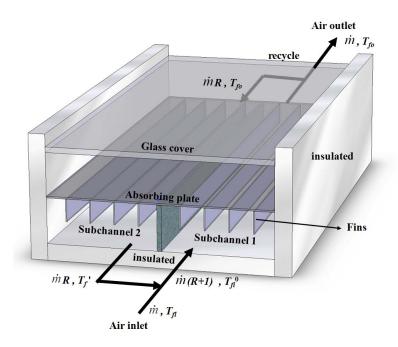
Solar air collector efficiency can be improved by enhancing the free and force convection effects [7,8], increasing the transfer area [9] and creating turbulence inside the flow channel with baffles [10], or with corrugated surfaces [11]. It was pointed out that applying the recycling effect to heat-and mass exchangers can effectively enhance performance due to the increase in fluid velocity, resulting in convective heat or mass transfer enhancement [12–17]. This work investigates collector efficiency in a downward-type internal-recycle flat-plate solar air heater with fins attached on the absorbing plate for improved performance.

2. Theoretical Analysis

A downward-type internal-recycle solar air heater with n fins attached on the absorbing plate is considered with a flow channel of width *B*, length *L*, and height *H*, as shown in Figure 1. An insulated plate with negligible thickness is placed vertical to the absorbing plate and bottom plate at the centerline to divide the flow channel into subchannels 1 and 2 of equal width *B*/2. A pump is installed for recycling the exiting fluid with reflux ratio *R* from the end of subchannel 1 into subchannel 2. During operation, before entering subchannel 1, the inlet airflow with mass flow rate $\dot{m}$ and

temperature T_{fi} will mix with the airflow exiting from subchannel 2 with mass flow rate $\dot{m}R$ and temperature T_f'. The following assumptions are made in this analysis: (1) the absorbing-plate, bottom-plate and bulk-fluid temperatures are functions of the flow direction (z) only; (2) both glass covers and fluid do not absorb radiant energy; (3) except for the glass covers all parts of the outside solar air collector surface, as well as the thin plate for separating both subchannels, are well thermally insulated; (4) the physical properties of the fluid and materials are constant; and (5) steady state operation exists.

Figure 1. Downward-type solar air collector with internal recycle and fins attached.

2.1. Temperature Distribution for the Fluid in Subchannel 1

The steady-state energy balance for differential sections of the absorbing plate, bottom plate and flowing fluid are, respectively:

$$I_0 \tau_g \alpha_p (B/2)dz - h_1\phi_1(B/2)dz(T_P - T_R) - h_{r,P-R}(B/2)dz(T_P - T_R) - U_t(B/2)dz(T_P - T_a) = 0 \tag{1}$$

$$h_{r,P-R}(B/2)dz(T_P - T_R) - h_1(B/2)dz(T_R - T_{f1}) = 0 \tag{2}$$

$$[m(1+R)C_P](dT_{f1}/dz)dz = h_1\phi_1(B/2)dz(T_P - T_{f1}) + h_1(B/2)dz(T_R - T_{f1}) \tag{3}$$

where:

$$\phi_1 = 1 + (A_f/A_c)\eta_{f,1} \tag{4}$$

in which A_f $(=2nw_2L)$ and A_c $(=BL)$ are the surface areas of n fins and absorbing plate, respectively, while $\eta_{f,1}$ denotes the fin efficiency in subchannel 1, *i.e.*, [18]:

$$\eta_{f,1} = (\tanh M_1 w_2)/Mw_2 \tag{5}$$

and:

$$M_1 = \sqrt{2h_1 / k_s t} \tag{6}$$

Solving Equations (1) and (2) for $(T_P - T_{f1})$ and $(T_R - T_{f1})$, we have:

$$T_P - T_{f1} = \frac{I_0 \tau_g \alpha_P (h_1 + h_{r,P-R}) - (h_1 U_t + h_{r,P-R} U_t)(T_{f1} - T_a)}{h_1 [h_1 \phi_1 + (1 + \phi_1) h_{r,P-R} + U_t] + h_{r,P-R} U_t} \tag{7}$$

$$T_R - T_{f1} = \frac{I_0 \tau_g \alpha_P h_{r,P-R} - h_{r,P-R} U_t (T_{f1} - T_a)}{h_1 [h_1 \phi_1 + (1 + \phi_1) h_{r,P-R} + U_t] + h_{r,P-R} U_t} \tag{8}$$

Substituting Equations (7) and (8) into Equation (3), one has:

$$[2m(1 + R)C_P]\frac{dT_{f1}}{dz} = BF_1 [I_0 \tau_g \alpha_P - U_t (T_{f1} T_a)] \tag{9}$$

where:

$$F_1 = \frac{h_1 [h_1 \phi + (1 + \phi_1) h_{r,P-R}]}{h_1 [h_1 \phi_1 + (1 + \phi_1) h_{r,P-R} + U_t] + h_{r,P-R} U_t} \tag{10}$$

in which F_1 is called the collector efficiency factor of subchannel 1, which is essentially constant for any design and fluid rate [3] and U_t is the loss coefficient from the solar collector top to the ambient air. If U_t is assumed to be constant along the flow direction, Equation (9) can be easily integrated for the boundary condition:

$$T_{f1} = T_{fi}^0 \text{ at } z = 0 \tag{11}$$

The result is:

$$\frac{T_{f1} - T_a - (I_0 \tau_g \alpha_P / U_t)}{T_{fi}^0 - T_a - (I_0 \tau_g \alpha_P / U_t)} = \exp\left[-\frac{F_1 U_t Bz}{2\dot{m}(1 + R)C_P}\right] \tag{12}$$

Equation (12) is the temperature distribution of the bulk fluid along the flow direction (z) of subchannel 1. Thus, the fluid temperature at the outlet of subchannel 1 is readily obtained from Equation (12) by substituting the condition:

$$T_{f1} = T_{fo} \text{ at } z = L$$

The result is:

$$\frac{T_{fo} - T_a - (I_0 \tau_g \alpha_P / U_t)}{T_{fi}^0 - T_a - (I_0 \tau_g \alpha_P / U_t)} = \exp\left[-\frac{F_1 U_t A_c}{2\dot{m}(1 + R)C_P}\right] \tag{13}$$

where $A_c = BL = nw_1 L$, surface area of the absorbing plate. Similarly, the differential energy-balance equation for the fluid in subchannel 2 is readily obtained using the same procedure performed for subchannel 1 except for the boundary conditions of $T_{f2} = T_f'$ at $z = 0$:

$$\frac{T_{fo} - T_a - (I_0 \tau_g \alpha_P / U_t)}{T_f' - T_a - (I_0 \tau_g \alpha_P / U_t)} = \exp\left[\frac{F_2 U_t A_c}{2\dot{m}RC_P}\right] \tag{14}$$

where the collector efficiency factor of subchannel 2 is defined as:

$$F_2 = \frac{h_2\left[h_2\phi_2 + (1+\phi_2)h_{r,P-R}\right]}{h_2\left[h_2\phi_2 + (1+\phi_2)h_{r,P-R} + U_t\right] + h_{r,P-R}U_t} \tag{15}$$

2.2. Mixed Inlet Temperature

If Equation (13) is divided by Equation (14), one has:

$$\frac{T_f' - T_a - \left(I_0\tau_g\alpha_P / U_t\right)}{T_{fi}^0 - T_a - \left(I_0\tau_g\alpha_P / U_t\right)} = \exp\left[-\frac{A_cU_t\{F_1R + F_2(1+R)\}}{2\dot{m}C_PR(1+R)}\right] \tag{16}$$

Taking energy balance at the inlet with T_{fi} as the reference temperature, this gives:

$$\dot{m}C_P(T_{fi} - T_{fi}) + \dot{m}RC_P(T_f' - T_{fi}) = \dot{m}(1+R)C_P(T_{fi}^0 - T_{fi}) \tag{17}$$

or:

$$T_f' = \frac{(1+R)T_{fi}^0 - T_{fi}}{R} \tag{18}$$

Substitution of Equation (18) is substituted into Equation (16) to eliminate T_f' resulting in the mixed inlet temperature as:

$$T_{fi}^0 = \frac{(T_{fi}/R) + [T_a + (I_o\tau_g\alpha_p / U_t]\{1 - \exp[-A_CU_t\{F_1R + F_2(1+R)\}/2\dot{m}C_PR(1+R)]\}}{[(1+R)/R] - \exp[-A_CU_t\{F_1R + F_2(1+R)\}/2\dot{m}C_PR(1+R)]} \tag{19}$$

2.3. Outlet Temperature and Collector Efficiency

Once the mixed inlet temperature is calculated from Equation (19), the outlet temperature T_{fo} in the downward-type internal-recycle solar air heaters with fins attached is readily obtained from Equation (13). The collector efficiency η_{cf} may be defined with the useful gain of energy Q_u divided by the insolation I_0A_c, as:

$$\eta_{cf} = Q_u/I_0A_c = \dot{m}C_P(T_{fo} - T_{fi})/I_0A_c \tag{20}$$

2.4. Mean Fluid and Absorbing Plate Temperatures

The mean fluid and absorbing-plate temperatures are needed for calculating the heat-transfer coefficients. The mean-fluid temperature may be taken approximately as:

$$T_{fm} = (T_{fi} + T_{fo})/2 \tag{21}$$

Substitution of Equation (20) is substituted into Equation (21) to eliminate T_{fo} giving T_{fm} in terms of η_{cf} as:

$$T_{fm} = T_{fi} + (\eta_{cf}I_0A_c/2\dot{m}C_P) \tag{22}$$

The collector efficiency may also be defined using:

$$\eta_{cf} = [I_0 A_c \tau_g \alpha_P - U_t A_c (T_{pm} - T_a)] / I_0 A_c$$

or:

$$\eta_{cf} = \tau_g \alpha_P - U_t (T_{pm} - T_a)/I_0 \qquad (23)$$

and the mean absorbing-plate temperature can be expressed in terms of η_{cf} as:

$$T_{pm} = T_a + I_0 U_t (\tau_g \alpha_P - \eta_{cf}) \qquad (24)$$

2.5. Heat Transfer Coefficients

The convective heat-transfer coefficient h_w for air flowing over the outside surface of the glass cover depends primarily on the wind velocity V. McAdams [14] obtained the experimental result as:

$$h_w = 5.7 + 3.8V \qquad (25)$$

An empirical equation for the loss coefficient from the top of the solar collector to the ambient U_t was developed by Klein [19] following the basic procedure of Hottel and Woertz [20] for the horizontal collector with one glass cover shown in Figure 1:

$$U_t = \left\{ \frac{(T_{pm}/520)}{\left[\frac{(T_{pm} - T_a)}{1 + (1 + 0.0059 h_w - 0.1166 h_w \varepsilon_p (1 + 0.7866 \times 1)} \right]^{0.34(1 - 100/T_m)}} + \frac{1}{h_w} \right\}^{-1}$$
$$+ \frac{\sigma(T_{pm} + T_a)(T_{pm}^2 + T_a^2)}{(\varepsilon_p + 0.00591 h_w \times 1)^{-1} + \left\{ [2 \times 1 + (1 + 0.089 h_w - 0.1166 h_w \varepsilon_p)(1 + 0.07866 \times 1) - 1 + 0.133 \varepsilon_p]/\varepsilon_p \right\} - 1} \qquad (26)$$

and Equation (26) can also be expressed in terms of thermal resistances for this single glass cover system from the collector plate to the ambient air as follows:

$$U_t = \left[\frac{1}{h_{p-c} + h_{r,p-c}} + \frac{1}{h_w + h_{r,c-a}} \right]^{-1} \qquad (27)$$

if the wind heat transfer coefficient h_w of ±10% uncertainty existed and the amount of change in the value of U_t was calculated within ±2% in the present study.

The radiation coefficient between the two air-duct surfaces may be estimated by assuming a mean radiant temperature equal to the mean fluid temperature [3], *i.e.*:

$$h_{r,P-R} = \frac{4 \sigma T_{fm}^3}{\frac{1}{\varepsilon_p} + \frac{1}{\varepsilon_R} - 1} \qquad (28)$$

In a solar air heater and collector-storage walls study it is necessary to know the forced convection heat-transfer coefficient between two flat plates. The following correlations [21] for air may be derived from Kay's data for fully developed turbulent flow with one side heated and the other side insulated:

$$Nu_1 = h_1 D_{eq,1}/k = 0.0158 \, Re_1 \tag{29}$$

$$Nu_2 = h_2 D_{eq,2}/k = 0.0158 \, Re_2 \tag{30}$$

The characteristic length is the equivalent diameter of the duct:

$$D_{eq,1} = D_{eq,2} = \frac{4H(B/2)}{2(H+B/2)} = \frac{2HB}{2H+B} \tag{31}$$

and the average air velocities in subchannels 1 and 2 are:

$$\bar{v}_1 = \frac{2\dot{m}(1+R)}{HB\rho} \tag{32}$$

$$\bar{v}_2 = \frac{2\dot{m}R}{HB\rho} \tag{33}$$

Thus, from Equations (31)–(33), one obtains the Reynolds numbers for the rectangular ducts as:

$$Re_1 = \frac{2\dot{m}(1+R)}{\mu(H+B/2)} \tag{34}$$

$$Re_2 = \frac{2\dot{m}R}{\mu(H+B/2)} \tag{35}$$

2.6. Calculation Method for η_{cf} and T_{fo}

The calculation procedure for the collector efficiency and outlet fluid temperature is now described. With known collector geometries (*L*, *B*, *H*) and system properties (τ_g, α_P, C_P, ρ, μ, k, k_s, ε_g, ε_p, ε_R), as well as the given operating conditions (I_0, T_a, V, $\dot{m}$, R, T_{fi}, n), a temporary value of η_{cf} is first estimated from Equation (20) using Equation (19) for T_{fo} once T_{fm} and T_{pm} are assumed. The T_{fm} and T_{pm} values are then checked using Equations (22) and (24), respectively, and new values of T_{fm} and T_{pm} may be obtained. If the calculated T_{fm} and T_{pm} values are different from the assumed values, continued calculation by iteration is needed until the last assumed values meet the finally calculated values, and thus the correct value of η_{cf}, as well as T_{fo}, is obtained. The following flow sheet may be helpful to simply expressing the calculation procedure.

Given:

$$\left.\begin{array}{l} \tau_g, \, \alpha_P, \, C_P, \, \rho, \, \mu, \, k, \, k_s, \, \varepsilon_g, \, \varepsilon_p \\ \varepsilon_R, I_0, \, T_a, \, V, \, \dot{m}, \, R, \, T_{fi}, \, n \end{array}\right\} \longrightarrow \left\{\begin{array}{l} \text{with } T_{fm} \text{ and} \\ T_{pm} \text{ assumed} \end{array}\right\} \xrightarrow[\text{Eq. (23)}]{\text{Eq. (22)}} \begin{array}{c} T_{fo} \\ \eta_{cf} \end{array} \xrightarrow[\text{Eq. (27)}]{\text{Eq. (25)}} \begin{array}{c} T_{fm} \\ T_{pm} \end{array} \longrightarrow \begin{array}{c} T_{fo} \\ \eta_{cf} \end{array} \tag{36}$$

iterations

3. Results and Discussion

3.1. Numerical Example

The improvement in performance of an internal-recycle double-pass solar air heater with *n* fins attached on the absorbing plate may be illustrated numerically using Table 1 and the following design
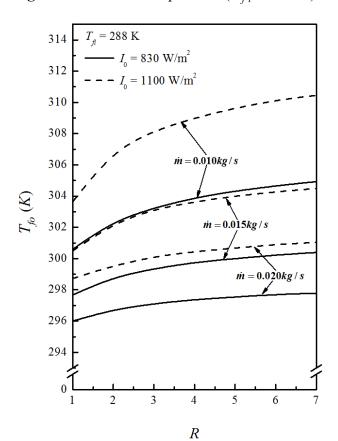
and operating conditions: $L = B = 0.6$ m; $A_c = LB = 0.36$ m^2; $H = 0.05$ m; $w_1 = 0.05$ m; $w_2 = 0.02$m; $t = 0.001$ m; $k_s = 45$ W/m K; $n = 12$; $\tau_g = 0.875$; $\alpha_p = 0.95$; $\varepsilon_g = 0.94$; $\varepsilon_p = 0.95$; $\varepsilon_R = 0.94$; $I_0 = 830$ and 1100 W/m^2; $T_{fi} = 288$, 293 and 298 K; $V = 1$ m/s; $\dot{m} = 0.01$, 0.015 and 0.02 kg/s; $T_a = 283$ K, $\sigma = 5.67 \times 10^{-8}$ W/m^{2}K^4. By substituting the specified values into the appropriate equations using Table 1 for the physical properties of the air, theoretical predictions for collector efficiency and outlet air temperature were obtained. The results are plotted in Figures 2–5. The most significant optical property affecting solar collector efficiency is the transmittance-absorptance product, *i.e.*, the numerical value $\tau_g \alpha_p = 0.95 \times 0.875 = 0.83125$ in the present study.

As an illustration showing the expected sensibility to the potential uncertainties, the transmittance-absorptance product of 5% uncertainty ($\tau_g \alpha_p = 0.87281$) was examined and the amount of changes of the value of T_{fo} was calculated by the procedure performed in Equation (36) and less than 0.5% in the present study with $T_{fi} = 288$ K, $I_0 = 830$ W/m^2, $\dot{m} = 0.01$ kg/s and $R = 1$.
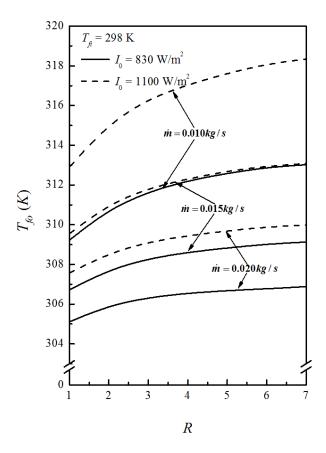
Table 1. Physical properties of air at 1 atm [3].

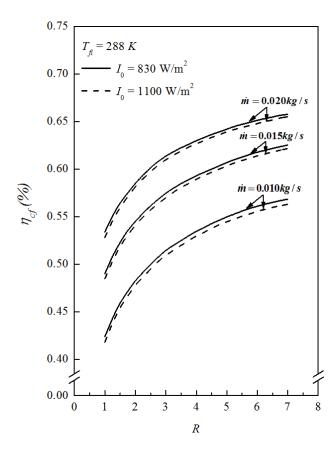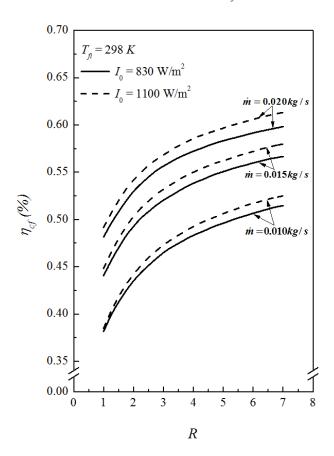| T (K)	ρ (kg/m^3)	C_p (J/kg · K)	k (W/kg · K)	μ (kg/m · s)
273	1.292	1006	0.0242	1.72×10^{-5}
293	1.204	1006	0.0257	1.81×10^{-5}
313	1.127	1007	0.0272	1.90×10^{-5}
333	1.059	1008	0.0287	1.99×10^{-5}
353	0.999	1010	0.0302	2.09×10^{-5}

Figure 2. Air outlet temperature ($T_{fi} = 288$K).

Figure 3. Air outlet temperature ($T_{fi} = 298K$).

Figure 4. Collector efficiency ($T_{fi} = 288K$).

Figure 5. Collector efficiency ($T_{f\,i} = 298\text{K}$).

3.2. Effects of Operating Parameters on Collector Efficiency

The outlet air temperature decreases when the air flow rate $\dot{m}$ increases and the collector efficiency increases, as indicated in Figures 2–5. On the other hand, the outlet air temperature T_{fo} increases with the inlet air temperature T_{fi}, resulting in a decrease in collector efficiency η_{cf}. Of course, both the outlet air temperature and collector efficiency increase when the incident solar radiation I_0 increases.

3.3. Improvement in Performance by Recycling

The improvements (I_f and I) in collector efficiencies (η_{cf} and η_c) using downward-type internal-recycle collectors with and without fins attached, respectively, are best illustrated by calculating the percentage increase in collector efficiency based on $\overline{\eta}_c$ obtained in a single-pass device of same size without recycling and fins attached, *i.e.*:

$$I_f = \frac{\text{collector efficiency of double-pass recycled device with fins}, \eta_{cf}}{\text{collector efficiency of single-pass device without recycling and fins}, \overline{\eta}_c} - 1 \qquad (37)$$

$$I = \frac{\text{collector efficiency of double-pass recycled device without fins}, \eta_c}{\text{collector efficiency of single-pass device without recycling and fins}, \overline{\eta}_c} - 1 \qquad (38)$$

The theoretical values of I_f for the system of present interest with the given values of $\overline{\eta}_c$ [17], were calculated using Equation (37), and the results are listed in Table 2. The predicted values for I

without attached fins were already calculated in a previous work [22]. The results are also presented in Table 2 for comparison. Operating with recycling substantially improves the collector efficiency with or without fins attached, as confirmed from this table and Figures 2–5. The improvements increase with increasing reflux ratio R, especially when operating at lower air flow rate $\dot{m}$ with higher inlet air temperature T_{fi}. For instance, the improvements in collector efficiency I_f in the recycled collector with fins attached, operating at $\dot{m} = 0.01\,\text{kg/s}$, $T_{fi} = 298\,\text{K}$ and $R = 5$, are 126.73% and 132.15% for $I_0 = 830$ and $1100\,\text{W/m}^2$, respectively. The contribution of increasing fluid velocity by applying the internal-recycle operation may be more effective than the undesirable effect of lowering the temperature difference by remixing.

3.4. Effect of Fin Attached on Performance

The improvements I in collector efficiency obtained in a downward-type internal-recycle recycled solar air heater of the same size but without fins attached [22], are also listed in Table 2 for comparison. Considerable further collector efficiency enhancement is achieved if fins are attached to the absorbing plate to increase the heat transfer area. Taking the case of $I_0 = 1100\,\text{W/m}^2$, $T_{fi} = 298\,K$, $\dot{m} = 0.01\,\text{kg/s}$, and $R = 1$ for example, more than 26% improvement ($I_f - I = 76.77 - 50.68\,\%$) is obtained when employing the device with fins attached, instead of using the same device but without fins employed in the previous work [22].

The further enhancement in collector efficiency E by attaching fins on the absorbing plate may be illustrated, based on a device of the same size but without fins, as:

$$E = \frac{\eta_{cf} - \eta_c}{\eta_c} \tag{39}$$

Equation (39) may be rewritten using Equations (37) and (38) as:

$$E = [\frac{(\eta_{cf} - \overline{\eta}_c) - (\eta_c - \overline{\eta}_c)}{\overline{\eta}_c}](\overline{\eta}_c / \eta_c) = (I_f - I)(\overline{\eta}_c / \eta_c) = \frac{I_f - I}{1 + I} \tag{40}$$

Some values for E were calculated from Table 2, with the results listed in Table 3. As shown in this table further collector efficiency enhancement in the device with fins attached increases with the inlet air temperature T_{fi}, while efficiency decreases when the reflux ratio R and/or the air flow rate $\dot{m}$ increases.

Table 2. The improvements of performance for: (**a**) $I_0 = 830 \text{ W/m}^2$; (**b**) $I_0 = 1100 \text{ W/m}^2$.

	T_{fi} (K)	$\dot{m}$ (kg/s)	η_0 (%)	I (%) (Yeh and Ho, [22])				I_f (%)			
				$R = 1$	$R = 3$	$R = 5$	$R = 7$	$R = 1$	$R = 3$	$R = 5$	$R = 7$
(**a**)	288	0.01	24.60	48.61	89.39	106.96	117.53	72.56	109.71	128.70	132.32
		0.015	30.35	41.42	74.32	88.06	96.23	61.65	90.32	101.02	106.96
		0.02	34.65	36.52	64.52	75.98	82.69	54.20	77.69	86.21	91.66
	293	0.01	23.28	48.66	89.56	107.27	117.90	73.37	110.91	125.47	133.76
		0.015	28.75	41.54	74.64	88.50	96.74	62.40	91.41	102.26	108.28
		0.02	32.84	36.67	64.89	76.46	83.25	54.94	78.78	87.46	92.21
	298	0.01	21.96	48.69	89.81	107.56	118.26	74.09	111.98	126.73	135.11
		0.015	27.14	41.64	74.95	88.91	97.23	63.16	92.93	103.50	109.62
		0.02	31.02	36.81	65.25	76.93	83.79	55.67	79.82	88.65	93.49
(**b**)	288	0.01	23.92	50.66	93.41	111.81	122.86	75.29	114.47	129.68	138.34
		0.015	29.73	43.17	77.48	91.80	100.31	63.91	94.01	105.21	111.47
		0.02	34.11	37.99	67.07	78.95	85.93	56.08	81.24	89.56	94.46
	293	0.01	22.90	50.68	93.52	112.05	123.16	76.03	115.54	130.91	139.61
		0.015	28.48	43.26	77.76	92.17	100.75	64.83	95.40	106.35	113.49
		0.02	32.69	38.11	67.39	79.38	86.43	56.81	81.68	90.73	95.72
	298	0.01	21.87	50.68	93.71	112.27	123.44	76.77	116.6	132.15	140.97
		0.015	27.21	43.34	78.02	92.53	101.17	65.42	96.14	107.68	114.11
		0.02	31.26	38.23	67.71	79.79	86.91	57.52	92.69	91.88	96.97

Table 3. Further enhancement of performance for: (**a**) $I_0 = 830 \text{ W/m}^2$; (**b**) $I_0 = 1100 \text{ W/m}^2$.

	T_{fi} (K)	$\dot{m}$ (kg/s)	E (%)			
			$R = 1$	$R = 3$	$R = 5$	$R = 7$
(**a**)	288	0.01	49.27	22.73	20.33	12.58
		0.015	48.84	21.53	14.72	11.15
		0.02	48.12	20.41	13.46	10.85
	293	0.01	50.78	23.04	16.97	13.45
		0.015	50.22	22.47	15.55	11.93
		0.02	49.82	21.41	14.39	10.76
	298	0.01	52.17	24.69	17.82	14.25
		0.015	51.68	23.99	16.41	12.74
		0.02	51.24	22.33	15.23	11.58
(**b**)	288	0.01	48.62	22.55	15.98	12.60
		0.015	48.04	21.33	14.41	11.13
		0.02	47.62	21.13	13.44	9.93
	293	0.01	50.02	23.55	16.03	13.36
		0.015	49.86	22.69	15.70	12.65
		0.02	49.07	21.20	14.30	10.75
	298	0.01	51.48	24.43	17.71	14.20
		0.015	50.75	23.22	16.37	12.79
		0.02	50.46	22.12	15.15	11.58

4. Conclusions

The performance in a downward-type solar air heater with internal recycling was investigated in the previous work [22]. In the present study the absorbing plate of this device was attached with fins for further improved performance.

In addition to the recycling operation, further enhancement in collector efficiency is obtainable if the operation is carried out with fins attached on the absorbing plate. Further enhancement in collector efficiency E based on the device without fins, reaches 51.48% for $I_0 = 1100$ W/m^2, $T_{fi} = 298$ K, $\dot{m} = 0.01$ kg/s and $R = 1$. Further enhancement in collector efficiency E decreases when the air flow rate and/or the reflux ratio increase. Therefore, employing fins on the absorbing plate is ineffective when the performance is operated under a large reflux ratio with high air flow rate.

The improvements in collector efficiencies, I_f and I, in the recycled devices with and without attached fins, increase with increasing reflux ratio, especially when operating at a lower air flow rate. It is shown in Table 2 and Figures 2–5 that the desirable effect of increasing the fluid velocity using the recycle operation compensates for the undesirable effect of decreasing the driving force (temperature difference) for heat transfer due to the remixing at the inlet. We can see in Table 2 that about 140% improvement I_f in collector efficiency is obtained by employing the recycled solar air heater with attached fins based on comparison with the single-pass device of same size operated without recycling and fins. The order of performances in the devices of same size is: double pass with recycle and fins > double pass with recycle but without fins > single pass without recycle and fins.

Acknowledgement

Conflicts of Interest

The authors declare no conflict of interest.

References

1. Gary, H.P.; Adhikari, R.S. Performance evaluation of a single solar air heater with n-subcollectors connected in different combinations. *Int. J. Energy Res.* **2000**, *23*, 403–414.
2. Belusko, M.; Saman, W.; Bruno, F. Performance of jet impingement in unglazed air collectors. *Sol. Energy* **2008**, *82*, 389–398.
3. Duffie, J.A.; Beckman, W.A. *Solar Engineering of Thermal Process*, 2nd ed.; Wiley: New York, NY, USA, 1991.
4. Tan, H.M.; Charter, W.S. Experimental investigation of force-convective heat transfer for fully-developed turbulent flow in a rectangular duct with asymmetric heating. *Sol. Energy* **1970**, *13*, 121–125.
5. Close, D.J.; Dunkle, R.V. Behaviour of absorbent energy storage beds. *Sol. Energy* **1976**, *18*, 287–292.
6. Seluck, M.K. *Solar Air Heater and Their Applications*; Sayigh, A.A.M., Ed.; Academic Press: New York, NY, USA; 1977.

7. Tonui, J.K.; Tripanagnostopoulos, Y. Improved PV/T solar collectors with heat extraction by force or natural air circulation. *Renew. Energy* **2007**, *32*, 623–637.

8. Yeh, H.M.; Ting, Y.C. Effects of free convection on collector efficiencies of solar air heaters. *Appl. Energy* **1986**, *22*, 145–155.

9. Mohamad, A.A. High efficiency solar air heater. *Sol. Energy* **1997**, *60*, 71–76.

10. Yeh, H.M. Theory of baffle solar air heaters. *Energy* **1992**, *17*, 692–702.

11. Gao, W.F.; Lin, W.X.; Lu, E.R. Numerical study on natural convection inside the channel between the flat plate cover and sine-wave absorber of a cross-corrugated solar air-heater. *Energy Convers. Manag.* **2000**, *41*, 145–151.

12. Ho, C.D.; Yeh, H.M.; Sheu, W.S. An analytical study of heat and mass transfer through a parallel-plate channel with recycle. *Int. J. Heat Mass Transf.* **1998**, *41*, 2589–2599.

13. Ho, C.D.; Yeh, H.M.; Sheu, W.S. The Influence of recycle on double-pass heat and mass transfer through a parallel-plate. *Int. J. Heat Mass Transf.* **1999**, *42*, 1707–1722.

14. McAdams, W.H. *Heat Transmission*, 3rd ed.; McGraw-Hill: New York, NY, USA, 1954.

15. Yeh, H.M.; Tsai, S.W.; Lin, C.S. A study of the separation efficiency in thermal diffusion column with a vertical permeable barrier. *AIChE J.* **1986**, *32*, 971–980.

16. Yeh, H.M.; Tsai, S.W.; Chiang, C.L. Recycle effects on heat and mass transfer through a parallel-plate channel. *AIChE J.* **1987**, *33*, 1743–1746.

17. Yeh, H.M.; Ho, C.D. Solar air heaters with external recycle. *App. Therm. Eng.* **2009**, *29*, 1694–1701.

18. Bennett, C.O.; Myers, J.E. *Momentum, Heat and Mass Transfer*, 2nd ed.; McGraw-Hill Inc.: New York, NY, USA, 1974; p.445.

19. Klein, S.A. Calculation of flat-plate loss coefficients. *Sol. Energy* **1975**, *17*, 79–80.

20. Hottel, H.C.; Woertz, B.B. Performance of flat-plate solar-heat collector. *Trans. ASME* **1942**, *64*, 91–104.

21. Kays, W.M.; Crawford, M.E. *Convective Heat- and Mass- Transfer*, 2nd ed.; McGraw-Hill: New York, NY, USA, 1980.

22. Yeh, H.M.; Ho, C.D. Downward-type solar air heaters with internal recycle. *J. Taiwan Inst. Chem. Eng.* **2011**, *42*, 286–291.